THE JOURNAL OF BIOLOGICAL CHEMISTRY Vol. 276, No. 32, Issue of August 10, pp. 30335–30341, 2001
Printed in U.S.A.

Early Intermediates in HIV-1 Envelope Glycoprotein-mediated Fusion Triggered by CD4 and Co-receptor Complexes*

Received for publication, April 27, 2001, and in revised form, June 6, 2001
Published, JBC Papers in Press, June 7, 2001, DOI 10.1074/jbc.M103788200

Antony S. Dimitrov, Xiaodong Xiao, Dimiter S. Dimitrov, and Robert Blumenthal‡

From the Laboratory of Experimental and Computational Biology, Center for Cancer Research, NCI, National Institutes of Health, Frederick, Maryland 21702

An early step in the process of HIV-1 entry into target cells is the activation of its envelope glycoprotein (GP120-GP41) to a fusogenic state upon binding to target cell CD4 and cognate co-receptor. Incubation of human immunodeficiency virus (HIV)-1 Env-expressing cells with an excess of CD4 and co-recepeptor-bearing target cells resulted in an influx of an impermeant nucleic acid-staining fluorescent dye into the Env-expressing cells. The dye influx occurred concomitant with cell fusion. No influx of dye into target cells was observed if they were incubated with an excess of Env-expressing cells. The permeabilization of Env-expressing cells was also triggered by CD4·co-receptor complexes attached to Protein G-Sepharose beads in the absence of target cells. The CD4 and co-receptor-induced permeabilization of Env-expressing cells occurred with the same specificity with respect to co-receptor usage as cell fusion. Natural ligands for the co-receptors and C-terminal GP41 peptide inhibitors of HIV-1 fusion blocked this effect. Our results indicate that the process of HIV-1 Env-mediated fusion is initiated by the destabilization of HIV-1 Env-expressing membranes. Further elucidation of these early intermediates may help identify and develop potential inhibitors of HIV-1 entry into cells.

HIV-1[1] enters susceptible cells by means of envelope glycoprotein-mediated fusion of viral and cellular membranes (1–4). The envelope glycoproteins are organized into oligomeric, probably trimeric spikes (5), and anchored in the viral membrane by the GP41 transmembrane protein. The surface of the spike, GP120, is associated by non-covalent interactions with each subunit of the trimeric GP41 (6). There are striking similarities between structural motifs in GP120-GP41 and influenza hemagglutinin (HA) leading to the notion that the native conformation of GP41 is metastable and it is stabilized by GP120 (7, 8). Host cell surface CD4 interacts with GP120-GP41 and causes conformational changes in GP120 that enables it to interact with a co-receptor, generally either CCR5 (R5) or CXCR4 (X4) (9–14). Coreceptor binding then triggers a barrage of additional conformational changes in the envelope glycoprotein (15) eventually resulting in the formation of a GP41 intermediate, dubbed a viral hairpin (16), which enables the GP41 to bring about the merging membranes (17, 18). The concept of the viral hairpin is based on the structure of the GP41 ectodomain core, which is a six-helix bundle composed of three helical hairpins, each consisting of an N helix paired with an antiparallel C helix (19–22). This structure shows similarity to the proposed fusogenic structures of envelope fusion proteins from influenza, Moloney murine leukemia virus, simian parainfluenza virus 5, Ebola virus, and simian immunodeficiency virus, as well to the snarepin fusion machinery involved in intracellular fusion events (23).

Many studies demonstrate that conformational changes in HIV-1 envelope glycoprotein can be induced by soluble CD4 (sCD4). For example, binding of sCD4 to the envelope glycoprotein complexes of particular HIV-1 strains results in dissociation of GP120 from the GP41 glycoprotein (24–27). Some of the variable loops (V1/V2 and V3) on the HIV-1 GP120 glycoprotein change conformation or become more exposed upon sCD4 binding, indicated by the enhanced binding of several anti-GP120 antibodies (28). Regions in GP120 that are exposed upon engagement of CD4 are involved in chemokine-receptor binding (29, 30).

The more drastic conformational changes leading to the viral hairpin have been more elusive. To capture GP41 following interaction of GP120-GP41 either with sCD4 or with cellular receptors, Weiss and co-workers (18) used a synthetic peptide, DP178 (39), corresponding to residues of the C helix in the GP41 core structure (19–22). DP178 tagged with an influenza HA epitope (178HA) binds to the N-terminal coiled coil of GP41 in a pre-hairpin conformation, which becomes available when the GP120 clamp is released. The 178HA presumably binds to the N-terminal coiled coil of GP41 in a pre-hairpin conformation, which becomes available when the GP120 clamp is released. Interestingly, in some viral isolates (notably HXB2) this conformation becomes available to DP178 following incubation with sCD4, whereas other isolates require cell surface-expressed CD4 and co-receptor to induce this intermediate.

In this study we have triggered conformational changes in HIV-1 Env by incubating HIV-1 Env-expressing cells with either an excess of target cells bearing CD4 and cognate co-receptor or with CD4·co-receptor complexes that were previously attached to beads (31). The results of this study suggest that a crucial step in the HIV-1 Env-mediated fusion cascade is the destabilization of the membranes bearing HIV-1 Env.

EXPERIMENTAL PROCEDURES

Cells Lines, Vaccinia Vectors, and Antibodies—HeLa, 293, and NIH 3T3 CD4 cells were cultured in Dulbecco's modified Eagle's medium (BIOSOURCE International, Camarillo, CA) containing 10% fetal bovine serum (Life Technologies Inc., Rockville, MD), NIH 3T3 CD4.X4 and NIH 3T3 CD4.R5 cell lines in Dulbecco's modified Eagle's medium, 10% fetal bovine serum with 3 μg/ml Puromycin. To express different HIV-1 Env the following recombinant vaccinia vectors were used: vSC60 and vPE16 (IIIB/Lai BH8 *env*), vCB43 (Ba-L *env*) (32), vPE17

* The costs of publication of this article were defrayed in part by the payment of page charges. This article must therefore be hereby marked "*advertisement*" in accordance with 18 U.S.C. Section 1734 solely to indicate this fact.

‡ To whom correspondence should be addressed: Center for Cancer Research, P.O. Box B, Bldg. 469, Rm. 216A, Miller Dr., Frederick, MD 21702-1201. Tel.: 301-846-1446; Fax: 301-846-6192; E-mail: blumen@helix.nih.gov.

[1] The abbreviations used are: HIV-1, human imunodeficiency virus-1; HA, hemagglutinin; GP, glycoprotein; sCD4, soluble CD4; mAb, monoclonal antibody; Env, envelope glycoprotein.

(IIIB/Lai BH8 *env* truncated at AA752 (33), and vPE12 (IIIB/Lai BH8 *env* with a deletion encompassing the GP120-GP41 cleavage site (33)). To express co-receptors, 293 cells were infected with pm1107 (vaccinia recombinant expressing CCR5) (31) or vvCXCR4 (34). The 5C7 mAb (anti-CCR5) was provided by Lijun Wu (35), OKT4 mAb (anti CD4) was a gift from Hana Golding, and 4G10 mAb (anti CXCR4) was a gift from Christopher Broder (34).

Expression of Vaccinia Recombinants—Experiments were performed in 35-mm coverslip bottom Petri dishes (MatTek Corp., Asland, MA), where 10^5 HeLa cells were plated 24 h prior the infection. The cells were infected with the appropriate recombinant vaccinia vectors at an multiplicity of infection of 3–5. Before infection, vaccinia stock (20 μl) was mixed with 30 μl of 0.25 mg/ml trypsin in phosphate-buffered saline, incubated at 37 °C for 30 min, diluted with 1 ml of Dulbecco's modified Eagle's medium + 2% fetal bovine serum and 100 μl of the vaccinia suspension was added to each well. After 2 h incubation at 37 °C, 2 ml of Dulbecco's modified Eagle's medium, 10% fetal bovine serum was added to each well and incubated for 12 h at 37 °C to express the respective GP120-GP41 envelope glycoproteins. The cells, kept at 31 °C, were able to fuse with appropriate target cells for 5 to 7 h after infection by vaccinia recombinants.

Preparation of CD4·Co-receptor Complexes—CD4·co-receptor complexes were attached to protein G-Sepharose beads using monoclonal antibodies and different cell lines: CD4.R5 beads were prepared from 3T3.CD4.R5 lysates and the 5C7 mAb (35), CD4.X4 beads from 3T3.CD4.X4 lysates and the 4G10 mAb (gift from Christopher Broder) (34), CD4 beads from 3T3.CD4 lysates and the OKT4 mAb (gift from Hana Golding), CCR5 beads from lysates of 293 cells which were infected with pm1107 (vaccinia recombinant expressing CCR5) (31) and the 5C7 mAb, CXCR4 beads from lysates of 293 cells infected with vvCXCR4 (34) and the 4G10 mAb, control beads from lysis buffer and the 5C7 mAb. The immunoprecipitation procedure was as described by Xiao and co-workers (31). The cells were washed with phosphate-buffered saline, lifted off using cell dissociation buffer, pelleted at 1500 rpm for 5 min, and resuspended at a final density of 10^7 cells/ml in lysis buffer, which contained 1% Brij-97, 150 mM NaCl, 20 mM Tris (pH 8.2), 20 mM EDTA, protease inhibitors (1 μg/ml each of leupeptin, aprotinin, and pepstanin), and 5 mM iodoacetamide. Incubation continued 1–3 h at 4 °C with gentle mixing. After the cell lysis, the cell nuclei were pelleted by centrifuging at 17,000 × *g* for 25 min in a refrigerated Eppendorf centrifuge. Then, 1.5–3 μg of immunoprecipitating antibodies and 15 μl of suspension of protein G-Sepharose beads (Sigma) prewashed with phosphate-buffered saline were added to each 1-ml supernatant. The beads were left overnight for 14 h at 4 °C on a rotator to bind the mAb and conjugated CD4/co-receptor. Then they were washed four times with ice-cold lysis iodoacetamide-free buffer and once with ice-cold phosphate-buffered saline, and aliquoted ready for use. The amount of CD4 attached to beads was quantitated by comparing the signal to that of a calibration curve from Western blots of known quantities of sCD4 (36).

Cell Fusion and Cell Membrane Permeabilization Assays—Calcein (485/525) and calcein blue (322/435) acetoxymethyl (AM) esters, and Sytox Orange (547/570) were all products from Molecular Probes (Eugene, OR). To monitor dye redistribution as a result of fusion HIV-1 Env-expressing cells and target cells were loaded with calcein-AM and calcein blue-AM, respectively, as described previously (17). The acetoxymethyl ester penetrates into the cells, where it is hydrolyzed to form the impermeant dye. Images of cells stained with the three dyes were acquired using an Olympus IX70 inverted fluorescent microscope equipped with an 82,000 filter cube from Chroma Technology Corp., a ×20 Ph1 PlanFluor objective (NA = 0.40), and Princeton Instrument, Inc. MicroMax cool CCD with 16-bit 1300 × 1300 pixel Interline chip. To perform kinetic experiments, the Env-expressing cells were washed 3 times with RPMI without serum, overlaid with 1 ml of 0.25 μg/ml Sytox Orange solution in RPMI (without serum), and the Petri dish was placed on the microscope stage thermostated at 37 °C. After reaching thermal equilibrium (within 10 min) about 5000 beads were added expressing CD4·co-receptor complex suspended in 100 μl of RPMI without serum. As the beads touched the cell layer images were acquired. The kinetics of Sytox Orange influx was recorded by acquiring and processing images every minute for 25 min after adding the beads, using MethaMorph 4.0 (Universal Imaging) software (15).

RESULTS

Influx of Dyes into HIV-1 Env-expressing Cells as a Result of Interactions with Susceptible Target Cells—In a previous study (15) we attempted to monitor CD4 and co-receptor-induced conformational changes of cell surface-expressed GP120-GP41 in the context of the fusion reaction using a fluorescent dye, which binds to hydrophobic groups. We reasoned that drastic changes in conformation would expose hydrophobic surfaces on GP120-GP41. Although the observed fluorescence changes maintained the specificity of the fusion reaction, we could not rule out the possibility that those changes are due to perturbations of the membranes of GP120-GP41-expressing cells. We explored this issue further using a high-affinity nucleic acid stain, Sytox Orange, which penetrates only cells with compromised plasma membranes. To provide a sufficient amount of CD4 and co-receptor to drive massive conformational changes in GP120-GP41 we incubated HIV-1_{IIIB}-expressing cells with an excess of NIH3T3.CD4.X4 target cells. Figs. 1, *B* and *C*, show redistribution of cytoplasmic dyes calcein blue and calcein green between target cells and Env-expressing cells as a result of HIV-1 Env-mediated cell fusion. In addition, an influx of Sytox Orange influx into the Env-expressing cells was observed when the target cells were added in excess of Env-expressing cells (Fig. 1*D*). Interestingly, the calcein blue and green had not completely leaked out of the fused cells, suggesting that the perturbations allowing Sytox influx may be transient. By contrast, when Env-expressing cells were incubated with an equivalent amount of target cells, we observed redistribution of the cytoplasmic dyes between Env-expressing cells and target cells as a result of HIV-1 Env-mediated cell fusion (Fig. 1, *F* and *G*), but no influx of Sytox Orange into either cell (Fig. 1*H*). Presumably there was a sufficient amount of CD4 and co-receptor available to drive fusion, without damage to the Env-expressing cells.

When Env-expressing cells were added in excess the redistribution of cytoplasmic dyes was observed (Fig. 1, *J* and *K*) without leakage from either target or effector cell (Fig. 1*L*). These data indicate that massive conformational changes induced in GP120-GP41 result in perturbation of the HIV-1 Env-expressing membrane. To characterize this phenomenon in more detail we used CD4 and co-receptor-associated beads to trigger the initial steps of the fusion reaction.

Interactions of CD4 and Co-receptor with HIV-1 Env-expressing Cells—Fig. 2 shows the relative amounts of CD4 complexed with CXCR4 or CCR5 attached to beads. Although the amount of CD4 in CD4 × 4 complexes is about 10 times reduced compared with the amount of CD4 in the CD4R5 complexes, these data allow us to quantify the response of GP120-GP41-expressing cells to these complexes at similar levels of CD4.

We monitored the Sytox fluorescence increase at 37 °C as a function of time. The fluorescence intensity is a measure of the rate of Sytox influx through the membrane and, hence, for the degree of membrane perturbation. Fig. 3 shows fluorescence changes in HIV-$1_{Ba\text{-}L}$ envelope glycoprotein-expressing cells, which occurred because of their interactions with CD4.R5 beads. After 12 min the fluorescence intensity is enhanced in cells, which surround the beads, and after 25 min all the cells in the field are stained with Sytox Orange. We also observe fluorescence increases in cells, which are not bound by beads. These are presumably due to the direct interaction between HIV-1 Env on the cells and CD4·co-receptor complexes, which dissociate from beads as a result of injection of a concentrated CD4/co-receptor/bead suspension at 4 °C into a dilute medium at 37 °C.

The integrated fluorescence from individual GP120-$GP41_{Ba\text{-}L}$-expressing cells was monitored at 37 °C as a function of time following addition of beads associated with the CD4.R5 complex or with CCR5 only (Fig. 4*A*). Each point represents an average of the intensities from 10 to 20 cells in the image area. The changes in the GP120-$GP41_{Ba\text{-}L}$-expressing cells induced

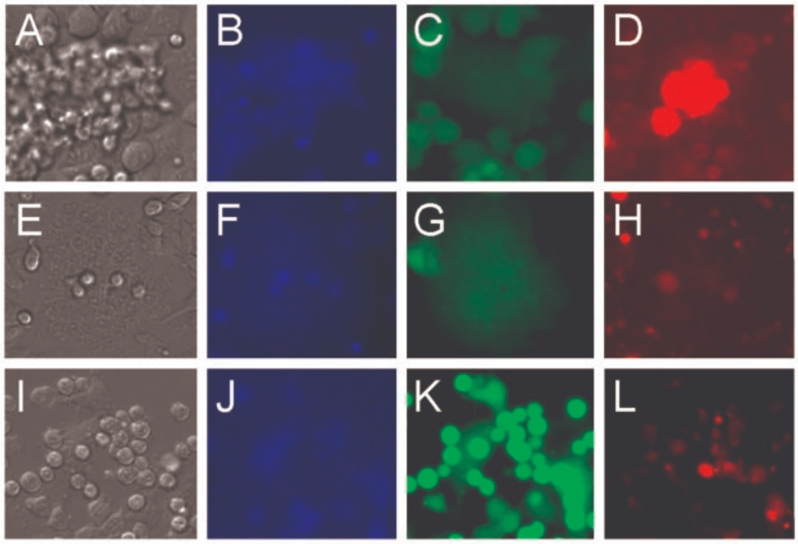

FIG. 1. **Influx of dyes into HIV-1 Env-expressing cells as a result of interactions with susceptible target cells HIV-1_{IIIB} Env-expressing cells, stained with calcein, were incubated for 2 h at 37 °C with NIH3T3.CD4.X4 cells, stained with calcein blue, in the presence of the impermeant nucleic acid stain, Sytox Orange in the medium.** The images were acquired in DIC (*A, E*, and *I*) and in fluorescence, using the "4,6-diamidino-2-phenylindole" (*B, F,* and *J*), "fluorescein isothiocyanate" (*C, G*, and *K*), and "rhodamine" (*D, H,* and *L*) optical filter cubes, respectively. Entry of Sytox into the cells is detected with the rhodamine filter cube. The experiment shown in *panels A-D* was performed with a NIH3T3.CD4.X4:HIV-1 Env-expressing cell ratio of about 5:1. The excess of target cells led to a severe destabilization of the membranes of the of the Env-expressing cell allowing Sytox to enter the intracellular compartments resulting in a sharp fluorescence increase (*panel D*). *Panels E-H* show a "normal" fusion process leading to syncytia formation when NIH3T3.CD4.X4 cells were added at ~1:1 to the Env-expressing cells. *Panels I-L* show dye transfer and fusion when Env-expressing cells were added in excess to plated NIH3T3.CD4.X4 cells. The lack of staining with Sytox in *panels H* and *L* (except for a few dead cells) indicates membrane fusion without leakage.

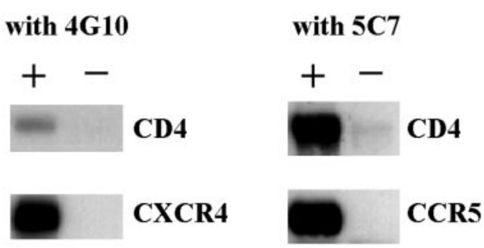

FIG. 2. **Co-immunoprecipitation of CD4.X4 and CD4.R5.** CD4 was co-immunoprecipitated with CXCR4 or CCR5 from lysates of NIH3T3.CD4.X4 (*left panel*) and NIH3T3.CD4.R5 (*right panel*) cells in the presence of the specific mAb to CXCR4 (4G10) and CCR5 (5C7), respectively, using Protein G-Sepharose beads. The *right side* of each panel (−) shows a negative control using lysates from NIH3T3.CD4 cells. Samples were run on a 10% SDS-polyacrylamide electrophoresis gel and Western blotting was performed using the T4–4 anti CD4 antibody (NIH AIDS R&RRP), a rabbit polyclonal anti-CXCR4 antibody (Biochain Institute, Hayward, CA), and a goat polyclonal anti-CCR5 antibody (Santa Cruz Biotechnology Inc., Santa Cruz, CA), respectively. The signal was detected using horseradish peroxidase-conjugated secondary antibodies, and the supersignal chemiluminescent substrate from Pierce (Rockford, Il). The images were acquired and quantified using a Bio-Rad PhosphorImager (Hercules, CA) at the highest resolution (0.1 mm). The amount of CD4 attached to beads was quantitated by comparing the signal to that of a calibration curve from Western blots of known quantities of sCD4. We estimated 5–15 ng of CD4 per 5000 CD4.R5 beads and 0.5–1.5 ng of CD4 per 5000 CD4.X4 beads for the experiments with optimal amounts of complex.

by CD4.R5 beads are rapid as compared with those seen with the CCR5 beads that do not trigger conformational changes in GP120-$GP41_{Ba-L}$ in the absence of CD4 (14). Fig. 4*B* shows that addition of sCD4, which did not cause a detectable effect, followed by addition of R5 beads did activate the GP120-$GP41_{Ba-L}$-expressing cells to a similar extent as compared with CD4.R5 beads. This is consistent with the reported activation of co-receptor-dependent fusion following incubation of HIV-1 envelope glycoprotein-expressing cells with sCD4 (14).

Fig. 5*A* shows the average fluorescence intensity per cell after 25 min of interaction of the beads with HeLa cells expressing the R5 utilizing envelope glycoprotein. The fluorescence intensity observed with beads with the highest amount of CD4.R5 was set to 100 and the intensities induced by the different receptor-associated beads were normalized with respect to that highest intensity. A 10-fold dilution of the level of CD4.R5 complexes on the beads leads to a 70% decrease in the fluorescence intensity induced in cells. Beads containing those complexes at a 100-fold lower amount showed a response in cells, which was close to the background. At similar levels of CD4, the CD4.R5 beads evoked a three times higher response in GP120-$GP41_{Ba-L}$-expressing cells than CD4.X4 beads. Conversely, in GP120-$GP41_{LAI}$-expressing cells, the response induced by CD4.X4 beads was 8 times higher as compared with that induced by CD4.R5 beads at similar levels of CD4·co-receptor complexes (Fig. 5*B*). Thus, the specificity of the response with respect to interactions of the GP120-GP41 with their cognate co-receptor is preserved in this assay.

Specificity of the Co-receptor-induced Perturbation of the Env-expressing Membrane—To further examine the specificity of the reaction we applied inhibitors of the GP120-chemokine receptor interaction and of HIV-1 envelope glycoprotein-mediated fusion. These include MIP-1β and RANTES, and SDF-1α, the natural ligands for CCR5 and CXCR4, respectively (37). We also examined the effects of synthetic C peptides (peptides corresponding to the C helix), which potently inhibit membrane fusion by both laboratory adapted strains and primary isolates of HIV-1 (38, 39), plausibly by interfering with the formation of the viral hairpin intermediate (18, 40). Fig. 6 shows that MIP-1β, inhibits the response induced by CD4.R5 beads in cells expressing the R5 utilizing envelope glycoprotein in a concentration-dependent manner. RANTES was somewhat less inhibitory: at 1 μg/ml RANTES showed around 30% decrease in the fluorescence response, whereas that concentration of MIP-1β inhibited more than 60%. By contrast, 1 μg/ml SDF-1α did not significantly decrease the CD4.R5-induced response. The peptide C34, which is a potent inhibitor of GP41 coiled-coil formation (41), inhibited the response in a concentration-dependent manner. This indi-

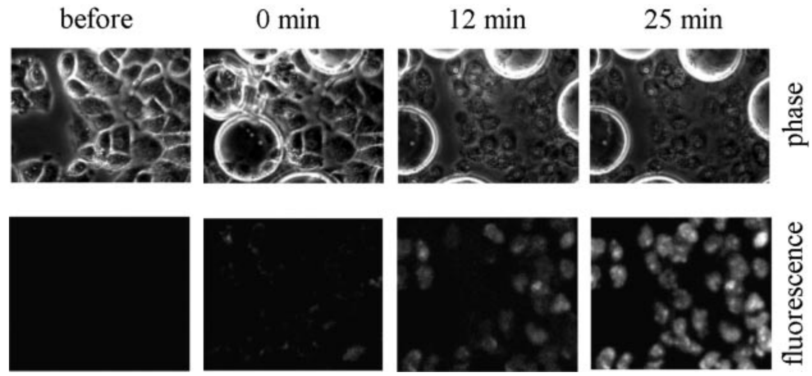

FIG. 3. **Sytox fluorescence in $GP120\text{-}GP41_{Ba\text{-}L}$-expressing HeLa cells before and after addition of CD4.R5 beads.** 5000 beads associated with CD4 (10 ng total) and CCR5 were added to the cells. Bright field (*top*) and Sytox fluorescent (λ_{ex} = 547, λ_{em} = 570) (*bottom*) were recorded before, 0, 12, and 25 min after adding the beads (*left* to *right*). Fluorescence increases observed after 25 min in cells, which are not bound by beads, are presumably due to CD4·co-receptor complexes, which became detached from the beads and interact directly with the HIV-1 Env on the cells.

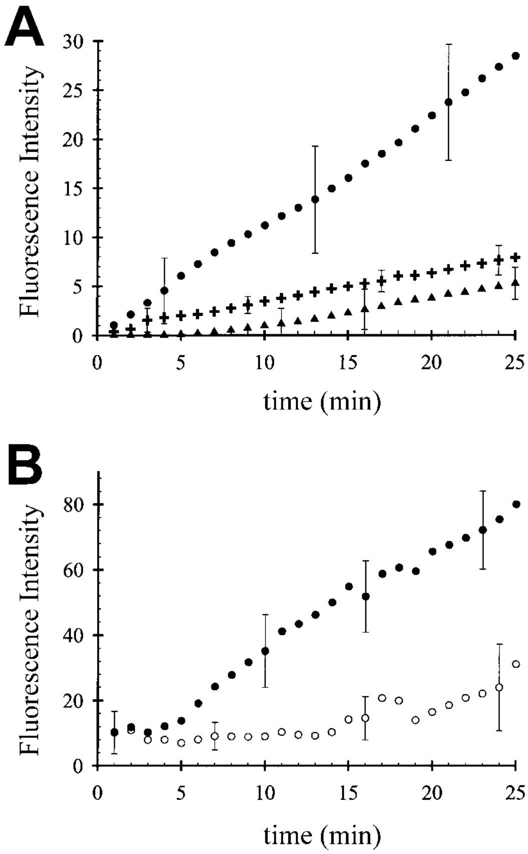

FIG. 4. **Kinetics of membrane permeabilization.** Sytox emission intensity changes upon addition of receptor-bearing beads to $GP120\text{-}GP41_{Ba\text{-}L}$-expressing HeLa cells. The points represent average changes in fluorescence intensity of 25–45 individual cells against time following addition of beads. For clarity *error bars* are shown only for a few data points. *A,* fluorescence changes upon addition of CD4.R5 beads (●) and R5 beads (+). ▲ represents background leakage of Sytox into the cells induced by control beads prepared from lysis buffer and the 5C7 mAb. *B,* fluorescence changes upon addition of sCD4 followed by R5 beads (●) and R5 beads without pre-addition of sCD4 (○). The *curves* represent the fluorescence after background subtraction of fluorescence changes induced by control beads. The addition of sCD4 did not induce fluorescence changes in the cells above those seen with "beads control."

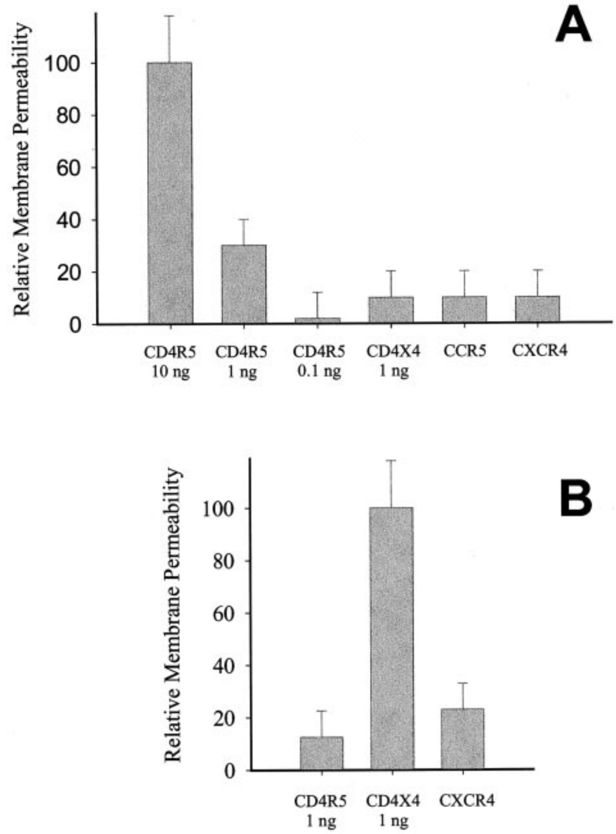

FIG. 5. **Effects of receptor concentration and inhibitors on CD4 and co-receptor-induced permeabilization of HIV-1 Env-expressing cells.** The relative membrane permeability is defined as $(F_s - F_n)/(F_p - F_n)$, where F_s, and F_p are average fluorescence intensities from the healthy cells after 25 min of incubation with beads complexed with a given amount and a maximum amount of CD4 and co-receptor, respectively, and F_n is the average fluorescence intensity from the healthy cells after 25 min of incubation with control beads prepared from lysis buffer and the 5C7 mAb. *A*, M-tropic $GP120\text{-}GP41_{Ba\text{-}L}$-expressing cells incubated with beads bound to the complexes as shown on the *abscissa*. The *number* next to the complex shows the average amount of CD4 in the experimental sample. *B*, T-tropic $GP120\text{-}GP41_{LAI}$-expressing cells incubated with beads bound to the complexes as shown on the *abscissa*.

cates that the changes in membrane permeability observed when CD4 and co-receptor bearing beads interact with cell surface-expressed GP120-GP41, occur as a result of GP41 coiled-coil formation. Interestingly, the concentration of peptide required for a similar inhibition of Sytox influx was about an order of magnitude higher in the case of DP178, which does not contain the amino acids that bind to the cavity formed by a cluster of residues in the N helix coiled coil (41) and interacts with the N-terminal peptides with low affinity (42).

The Effect of the Cytoplasmic Domain of GP41—Three amphipatic α-helices in the cytoplasmic domain of GP41 have been shown to perturb lipid bilayers (44–46). To examine the possibility that conformational changes induced in the extracytoplasmic domain of GP120-GP41 may lead to perturbations due to secondary associations of these "lytic peptides" with the inner leaflet of the plasma membrane we used a $GP120\text{-}GP41_{LAI}$ construct truncated at amino acid 752 (33), which does not contain any of the lytic peptide sequences but is still fusion competent. Fig. 7 shows a similar effect with the truncated GP41 to that seen with the full-length GP41, indicating that

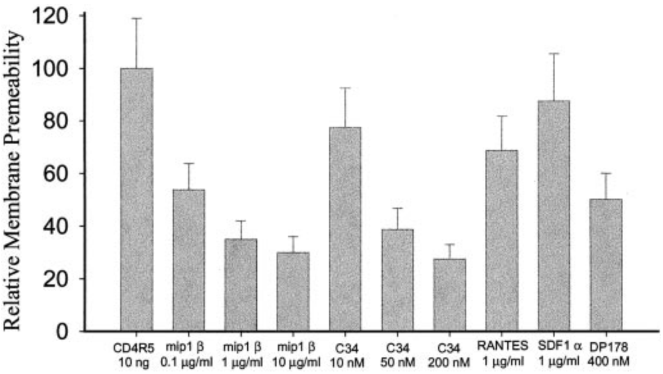

FIG. 6. **Effect of inhibitors and their concentration on the Sytox influx into GP120-GP41$_{Ba-L}$-expressing cells induced by CD4.R5 beads.** The relative membrane permeability is defined as $(F_s - F_n)/(F_p - F_n)$, where F_s, and F_p are average fluorescence intensities from the healthy cells after 25 min of incubation with beads complexed with CD4 (10 ng) and CCR5 in the presence and absence of reagent, respectively, and F_n is the average fluorescence intensity from the healthy cells after 25 min of incubation with control beads prepared from lysis buffer and the 5C7 mAb. The *abscissa* show the various reagents and their respective concentrations.

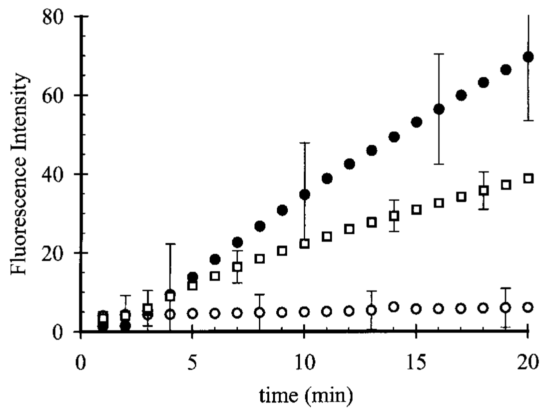

FIG. 7. **Effects of Env structure on CD4 and co-receptor-induced permeabilization of HIV-1 Env-expressing cells.** The experiments were performed as described in the legend to Fig. 4 with CD4·X4 beads added to HeLa cells expressing HIV-1 $_{IIIB}$ env which was unmodified (●), truncated at AA752 (○), and with a deletion encompassing the GP120-GP41 cleavage site (□).

certain peptides corresponding to sequences in the extra-cytoplasmic domain of HIV-1 Env are responsible for the observed change in membrane permeability. Fig. 7 shows that HIV-1 Env with a deletion mutation of the GP120-GP41 cleavage site did not produce the effect, indicating that fusion-active GP120-GP41 is required.

DISCUSSION

In this study, we show that interactions of Env-expressing cells with an excess of CD4 and co-receptor-bearing target cells results in the influx of the impermeant dye Sytox into the Env-expressing cells (Fig. 1). The Sytox influx occurs concomitantly with HIV-1 Env-mediated cell fusion as shown by redistribution of cytoplasmic dyes between target and effector cells. No Sytox influx was observed into the target cells even when incubated with an excess of Env-expressing cells. When the interactions between GP120-GP41, CD4, and co-receptors leading to fusion are limited, minor membrane perturbations are induced at the region of cell-cell contact and the Sytox influx is not observed. Since only a small number of activated Envs are required to drive HIV-1 Env-mediated fusion (47, 48), generally fusion will not be accompanied by leakage. The fact that the concentrations of C-terminal GP41 peptides required to inhibit CD4 and co-receptor-induced leakage (Fig. 6) are higher than those required to inhibit HIV-1 Env-mediated fusion (43) is consistent with the notion that fewer Envs need to be activated for the latter process. However, driving the fusion reaction to an undesired outcome (from the viral entry point of view) revealed an important intermediate, which sheds light on the overall mechanism of HIV-1 Env-mediated fusion.

Using CD4 and co-receptor-bearing beads we have measured the kinetics of this first step in the HIV-1 fusion reaction (Figs. 3 and 4). The CD4 and co-receptor-induced permeabilization of Env-expressing cells occurred with the same specificity with respect to co-receptor usage as cell fusion (Fig. 5). Natural ligands for the co-receptors and C-terminal GP41 peptide inhibitors of HIV-1 fusion blocked this effect (Fig. 6). While the extent of colocalization of CD4 and co-receptor in cells is very limited in the absence of GP120 (49) we were able to attach sufficient amounts of the complexes to beads (Fig. 2) to trigger the fusion reaction. Silver staining of proteins immunoprecipitated by the anti-CCR5 mAb 5C7 showed bands that are not specific to CCR5, because they were immunoprecipitated in CCR5-negative cells (31). However, control experiments with beads attached to the mAB 5C7 containing lysates from cells infected with vaccinia CCR5 or CXCR4 recombinants showed background responses (Figs. 4 and 5) when added to appropriate Env-expressing cells indicating that these contaminants do not contribute to destabilization of Env-expressing membranes. We also excluded the possibility that lipids are present on the bead surface by incorporating bodipy-labeled fluorescent fatty acids into the cells, which become metabolically transformed into phospholipids and glycosphingolipids (43, 50). Preparation of beads from these cells showed no fluorescence associated with beads indicating absence of lipids. We can therefore rule out the possibility that the observed increased permeability is due to fusion of Env-expressing cells with portions of CD4-chemokine receptor containing membranes attached to beads.

Although the 4G10 and 5C7 mAbs recognize the extracellular domains of the respective co-receptors, the CD4 and co-receptor-attached beads interact with GP120 in a predicted fashion in that GP120 binds specifically to its cognate co-receptor and sCD4 binds to co-receptor attached beads. To attach the C-terminal end of the co-receptor to beads, we have used C9-tagged CCR5 stably expressed in Cf2Th canine thymocytes (51). Beads attached to the 1D4 antibody, which binds C9 tagged-CCR5-CD4 complex, produced similar responses when added to HIV-1$_{Ba-L}$-Env-expressing cells as those seen in Figs. 3 and 4.

How do conformational changes triggered by CD4 and co-receptor cause membrane de-stabilization? The simplest explanation is that the triggering causes a release of the GP41 fusion peptide from a buried position within the GP120-GP41 trimer allowing it to insert into the envelope glycoprotein-expressing membrane. This notion is based on the striking similarities between structural motifs in GP120-GP41 and influenza HA (7, 8). Although it is generally assumed that the fusion peptide inserts into the target membrane following its release from inside the stem (2, 3), a number of models hypothesize that the interaction of the fusion peptides with the viral membrane is a necessary step of the fusion process (52–54). In the case of influenza HA, evidence for self-insertion of fusion peptides comes from photolabeling studies (55) and electron microscopic observations (56). Our data indicate that the interaction of cell surface-expressed GP120-GP41 with CD4 and cognate co-receptor attached to beads brings about a de-stabilization of the membrane expressing its own GP120-GP41, presumably due to self-insertion of the fusion peptide. Relocation of the fusion peptide to the target membrane following the CD4 and co-receptor-induced conformational changes in GP120-GP41 would initiate de-stabilization of the target, rather than the GP120-GP41-expressing bilayer. Our studies, however, reveal that de-stabilization of the envelope-expressing membrane occurs at an early stage of the HIV-1 cell fusion reaction. A number of studies with synthetic fusion peptides from the N-terminal sequence of HIV-1 GP41 indicate that they are capable of destabilizing membranes causing the release of lipid vesicle contents (57–60). They have been shown to induce lysis of intact human erythrocytes and $CD4^+$ lymphocytes (61). We have also observed that adding a synthetic HIV-1 GP41 fusion peptide at concentrations less than 1 μg/ml to cultured cells results in Sytox influx into these cells. The insertion of the peptide into the outer monolayer of the membrane presumably results in a rapid expansion of the area of the outer monolayer (62, 63). The bending stress of the outer monolayer may be relieved by rapid flip-flop of phospholipid (64) and peptide from outer to inner monolayer followed by the formation of nanometer-scale pores.

The self-insertion models, which have been developed for influenza HA, could readily be applied to GP120-GP41. According to the model proposed by Kozlov and Chernomordik (53), insertion of the fusion peptide into the viral membrane is followed by re-folding of the HA2 core into a trimeric coiled coil, which exerts forces that pull the membrane-associated fusion peptides. The elastic energy derived from the bending of the membrane around HA trimer into a saddle-like shape then drives self-assembly of these trimers. As a result, the viral envelope glycoprotein-expressing membrane will form a dimple within a ring-like cluster of HA2 coiled coils bulging out toward the bound target membrane. Bending stresses in the lipidic top of the dimple will cause local de-stabilization and facilitate membrane fusion. In addition, according to a hypothesis proposed Bentz (54), a second barrage of conformation changes may result in the expulsion of the fusion peptide and the creation of a hydrophobic defect in the Env-expressing membrane leading to three possible outcomes. 1) Recruitment of lipid from the outer monolayer of the target membrane will result in fusion. 2) Lipid flip-flop from the inner monolayer of the viral envelope glycoprotein-expressing membrane will result in leakage. 3) Lateral diffusion of lipids from the outer monolayer of the viral envelope glycoprotein-expressing membranes will result in healing and no changes are observed. Thus, by forcing the system into a pathway which is unfavorable for HIV-1 entry we have revealed an important intermediate in the HIV-1 fusion cascade.

Acknowledgments—We are grateful to Drs. H. Golding, P. Earl, L. Wu, C. Broder, V. Kewalramani, D. Littman, and NIH AIDS Research and Reference Reagent Program for the supply of cell lines and reagents. We also thank Drs. Thomas Korte, Anu Puri, Mathias Viard, Steve Gallo, and Yossef Raviv for fruitful discussions and continuous help during this study.

REFERENCES

1. Wyatt, R., and Sodroski, J. (1998) *Science* **280,** 1884–1888
2. Weissenhorn, W., Dessen, A., Calder, L. J., Harrison, S. C., Skehel, J. J., and Wiley, D. C. (1999) *Mol. Membr. Biol.* **16,** 3–9
3. Chan, D. C., and Kim, P. S. (1998) *Cell* **93,** 681–684
4. Dimitrov, D. S. (2000) *Cell* **101,** 697–702
5. Weiss, C. D., Levy, J. A., and White, J. M. (1990) *J. Virol.* **64,** 5674–5677
6. Kowalski, M., Potz, J., Basiripour, L., Dorfman, T., Goh, W. C., Terwilliger, E., Dayton, A., Rosen, C., Haseltine, W., and Sodroski, J. (1987) *Science* **237,** 1351–1355
7. Gallaher, W. R., Ball, J. M., Garry, R. F., Griffin, M. C., and Montelaro, R. C. (1989) *AIDS Res. Hum. Retroviruses* **5,** 431–440
8. Kwong, P. D., Wyatt, R., Sattentau, Q. J., Sodroski, J., and Hendrickson, W. A. (2000) *J. Virol.* **74,** 1961–1972
9. Berger, E. A. (1997) *AIDS* **11,** Suppl. A, S3–16
10. Doms, R. W., and Peiper, S. C. (1997) *Virology* **235,** 179–190
11. Moore, J. P., Trkola, A., and Dragic, T. (1997) *Curr. Opin. Immunol.* **9,** 551–562
12. Kwong, P. D., Wyatt, R., Robinson, J., Sweet, R. W., Sodroski, J., and Hendrickson, W. A. (1998) *Nature* **393,** 648–659
13. Zhang, W., Canziani, G., Plugariu, C., Wyatt, R., Sodroski, J., Sweet, R., Kwong, P., Hendrickson, W., and Chaiken, I. (1999) *Biochemistry* **38,** 9405–9416
14. Salzwedel, K., Smith, E. D., Dey, B., and Berger, E. A. (2000) *J. Virol.* **74,** 326–333
15. Jones, P. L., Korte, T., and Blumenthal, R. (1998) *J. Biol. Chem.* **273,** 404–409
16. Weber, T., Zemelman, B. V., McNew, J. A., Westermann, B., Gmachl, M., Parlati, F., Sollner, T. H., and Rothman, J. E. (1998) *Cell* **92,** 759–772
17. Munoz-Barroso, I., Durell, S., Sakaguchi, K., Appella, E., and Blumenthal, R. (1998) *J. Cell Biol.* **140,** 315–323
18. Furuta, R. A., Wild, C. T., Weng, Y., and Weiss, C. D. (1998) *Nat. Struct. Biol.* **5,** 276–279
19. Chan, D. C., Fass, D., Berger, J. M., and Kim, P. S. (1997) *Cell* **89,** 263–273
20. Weissenhorn, W., Dessen, A., Harrison, S. C., Skehel, J. J., and Wiley, D. C. (1997) *Nature* **387,** 426–428
21. Tan, K., Liu, J., Wang, J., Shen, S., and Lu, M. (1997) *Proc. Natl. Acad. Sci. U. S. A.* **94,** 12303–12308
22. Caffrey, M., Cai, M., Kaufman, J., Stahl, S. J., Wingfield, P. T., Covell, D. G., Gronenborn, A. M., and Clore, G. M. (1998) *EMBO J.* **17,** 4572–4584
23. Skehel, J. J., and Wiley, D. C. (1998) *Cell* **95,** 871–874
24. Moore, J. P., McKeating, J. A., Weiss, R. A., and Sattentau, Q. J. (1990) *Science* **250,** 1139–1142
25. Dimitrov, D. S., Hillman, K., Manischewitz, J., Blumenthal, R., and Golding, H. (1992) *AIDS* (*Phila.*) **60,** 249–256
26. Thali, M., Furman, C., Helseth, E., Repke, H., and Sodroski, J. (1992) *J. Virol.* **66,** 5516–5524
27. Fu, Y. K., Hart, T. K., Jonak, Z. L., and Bugelski, P. J. (1993) *J. Virol.* **67,** 3818–3825
28. Sullivan, N., Sun, Y., Sattentau, Q., Thali, M., Wu, D., Denisova, G., Gershoni, J., Robinson, J., Moore, J., and Sodroski, J. (1998) *J. Virol.* **72,** 4694–4703
29. Trkola, A., Dragic, T., Arthos, J., Binley, J. M., Olson, W. C., Allaway, G. P., Cheng-Mayer, C., Robinson, J., Maddon, P. J., and Moore, J. P. (1996) *Nature* **384,** 184–187
30. Wu, L., Gerard, N. P., Wyatt, R., Choe, H., Parolin, C., Ruffing, N., Borsetti, A., Cardoso, A. A., Desjardin, E., Newman, W., Gerard, C., and Sodroski, J. (1996) *Nature* **384,** 179–183
31. Xiao, X., Wu, L., Stantchev, T. S., Feng, Y. R., Ugolini, S., Chen, H., Shen, Z., Riley, J. L., Broder, C. C., Sattentau, Q. J., and Dimitrov, D. S. (1999) *Proc. Natl. Acad. Sci. U. S. A.* **96,** 7496–7501
32. Broder, C. C., and Berger, E. A. (1995) *Proc. Natl. Acad. Sci. U. S. A.* **92,** 9004–9008
33. Earl, P. L., Koenig, S., and Moss, B. (1991) *J. Virol.* **65,** 31–41
34. Chabot, D. J., Chen, H., Dimitrov, D. S., and Broder, C. C. (2000) *J. Virol.* **74,** 4404–4413
35. Wu, L., Paxton, W. A., Kassam, N., Ruffing, N., Rottman, J. B., Sullivan, N., Choe, H., Sodroski, J., Newman, W., Koup, R. A., and Mackay, C. R. (1997) *J. Exp. Med.* **185,** 1681–1691
36. Xiao, X., Norwood, D., Feng, Y. R., Moriuchi, M., Jones-Trower, A., Stantchev, T. S., Moriuchi, H., Broder, C. C., and Dimitrov, D. S. (2000) *Exp. Mol. Pathol.* **68,** 139–146
37. Baggiolini, M. (1998) *Nature* **392,** 565–568
38. Jiang, S., Lin, K., Strick, N., and Neurath, A. R. (1993) *Biochem. Biophys. Res. Commun.* **195,** 533–538
39. Wild, C. T., Shugars, D. C., Greenwell, T. K., McDanal, C. B., and Matthews, T. J. (1994) *Proc. Natl. Acad. Sci. U. S. A.* **91,** 9770–9774
40. Chen, C. H., Matthews, T. J., McDanal, C. B., Bolognesi, D. P., and Greenberg, M. L. (1995) *J. Virol.* **69,** 3771–3777
41. Chan, D. C., Chutkowski, C. T., and Kim, P. S. (1998) *Proc. Natl. Acad. Sci. U. S. A.* **95,** 15613–15617
42. Lawless, M. K., Barney, S., Guthrie, K. I., Bucy, T. B., Petteway, S. R., Jr., and Merutka, G. (1996) *Biochemistry* **35,** 13697–13708
43. Kliger, Y., Gallo, S. A., Peisajovich, S. G., Munoz-Barroso, I., Avkin, S., Blumenthal, R., and Shai, Y. (2001) *J. Biol. Chem.* **276,** 1391–1397
44. Miller, M. A., Cloyd, M. W., Liebmann, J., Rinaldo, C. R. J., Islam, K. R., Wang, S. Z., Mietzner, T. A., and Montelaro, R. C. (1993) *Virology* **196,** 89–100
45. Srinivas, S. K., Srinivas, R. V., Anantharamaiah, G. M., Segrest, J. P., and Compans, R. W. (1992) *J. Biol. Chem.* **267,** 7121–7127
46. Kliger, Y., and Shai, Y. (1997) *Biochemistry* **36,** 5157–5169
47. Freed, E. O., Delwart, E. L., Buchschacher, G. L., Jr., and Panganiban, A. T. (1992) *Proc. Natl. Acad. Sci. U. S. A.* **89,** 70–74
48. Kuhmann, S. E., Platt, E. J., Kozak, S. L., and Kabat, D. (2000) *J. Virol.* **74,** 7005–7015
49. Singer, I. I., Scott, S., Kawka, D. W., Chin, J., Daugherty, B. L., DeMartino, J. A., DiSalvo, J., Gould, S. L., Lineberger, J. E., Malkowitz, L., Miller, M. D., Mitnaul, L., Siciliano, S. J., Staruch, M. J., Williams, H. R., Zweerink, H. J., and Springer, M. S. (2001) *J. Virol.* **75,** 3779–3790
50. Kasurinen, J. (1992) *Biochem. Biophys. Res. Commun.* **187,** 1594–1601
51. Mirzabekov, T., Bannert, N., Farzan, M., Hofmann, W., Kolchinsky, P., Wu, L., Wyatt, R., and Sodroski, J. (1999) *J. Biol. Chem.* **274,** 28745–28750
52. Guy, H. R., Durell, S. R., Schoch, C., and Blumenthal, R. (1992) *Biophys. J.* **62,** 95–97
53. Kozlov, M. M., and Chernomordik, L. V. (1998) *Biophys. J.* **75,** 1384–1396
54. Bentz, J. (2000) *Biophys. J.* **78,** 886–900
55. Weber, T., Paesold, G., Galli, C., Mischler, R., Semenza, G., and Brunner, J. (1994) *J. Biol. Chem.* **269,** 18353–18358
56. Wharton, S. A., Calder, L. J., Ruigrok, R. W., Skehel, J. J., Steinhauer, D. A.,

and Wiley, D. C. (1995) *EMBO J.* **14,** 240–246
57. Rafalski, M., Lear, J. D., and DeGrado, W. F. (1990) *Biochemistry* **29,** 7917–7922
58. Nieva, J. L., Nir, S., Muga, A., Goni, F. M., and Wilschut, J. (1994) *Biochemistry.* **33,** 3201–3209
59. Slepushkin, V. A., Melikyan, G. B., Sidorova, M. S., Chumakov, V. M., Andreev, S. M., Manulyan, R. A., and Karamov, E. V. (1990) *Biochem. Biophys. Res. Commun.* **172,** 952–957
60. Kliger, Y., Aharoni, A., Rapaport, D., Jones, P., Blumenthal, R., and Shai, Y. (1997) *J. Biol. Chem.* 13496–13505
61. Mobley, P. W., Curtain, C. C., Kirkpatrick, A., Rostamkhani, M., Waring, A. J., and Gordon, L. M. (1992) *Biochim. Biophys. Acta* **1139,** 251–256
62. Longo, M. L., Waring, A. J., and Hammer, D. A. (1997) *Biophys. J.* **73,** 1430–1439
63. Blumenthal, R., and Morris, S. J. (1999) *Mol. Membr. Biol.* **16,** 43–47
64. Raphael, R. M., and Waugh, R. E. (1996) *Biophys. J.* **71,** 1374–1388